

# Pixel - based Wake Interaction and Power Estimation for a Wind Farm with Irregular Boundary

Gyde Ohlsen<sup>2,1</sup>, Oscar Ruiz-Salguero<sup>1</sup>, Thomas Full<sup>3,1</sup>, Diego Acosta<sup>4</sup>

<sup>1</sup>Laboratory of CAD CAM CAE, Universidad EAFIT, Colombia

<sup>2</sup>Department of Wind Energy, Technical University Denmark

<sup>3</sup>Institute of Materials Resource Management, Augsburg Universitaet, Germany

<sup>4</sup>Process Development and Design Group, Universidad EAFIT, Colombia

## Abstract

In the domain of generation of wind turbine energy, it is central to correctly estimate the interactions among the various turbines in a wind turbine farm. The spatial super-position of turbine wind wakes determines the wind conditions that each turbine in the farm is exposed to and its power output. The current state of the art represents the turbine wakes as a 2D real-valued polygonal trapezoid. The interactions among wakes imply Boolean operations among many trapezoids, producing an intractable fragmentation of the wake intersection and domain regions. The plan (2D) view of the terrain with this wake polygon fragmentation is then used to estimate the effective wind that each turbine receives. This calculation leads to cumbersome computation, which is even more impractical if 3D representations of the terrain, wakes and wind are needed. In response to these limitations, this manuscript presents a method in which the 2D turbine wakes are located on a terrain with holes and exclusion zones bounded by 2D polygons, considering wind direction and turbine array basic specifications. Then, a discretized or pixel approximation of the terrain and wake superposition is calculated using discrete levels of the turbine velocity deficits. This process allows a practical approximation of the power output of each turbine and of the full turbine set. The wake interaction and terrain boundaries are then texture - mapped onto the 3D representation of the terrain, for visualization purposes. As an application, an example of a complex polygonal terrain turbine farm is optimized for maximal power output. This discrete, image - based calculation is particularly convenient in a circumstance in which graphics hardware and GPU processors become increasingly available and efficient, in laptop and mobile devices. This investigation opens research opportunities in mixtures of turbine types, 3D modeling of wind / terrain interaction, and accelerated calculation and visualization with GPU hardware.

## Glossary

TIN	Triangulated Irregular Network, used for terrain description.
DOCE:	Design of Computer Experiments.
$M$	3D Terrain in TIN format.
$S$	Set of turbine positions $S = \{p_1, p_2, \dots\}$ with $p_i \in \Pi$
$\hat{i}$	iso-latitude unit vector at the turbine fram (earth parallel).
$\Pi$	Plane locally tangent to the iso-altitude surface at the turbine farm, equipped with X axis (iso-latitude) and Y axis (iso-longitude).
$\Gamma$	Set of closed Jordan curves on $\Pi$ . $\Gamma = \{\Gamma_0, \Gamma_1, \dots\}$ , with $\Gamma_0$ expressing the outermost wind farm boundary and $\Gamma_i$ denoting its $i$ -th internal hole (or excluded region).
$\Omega$	Useful 3D surface of the wind farm. Subset of $M$ ( $\Omega \subset M$ ) bounded by the projection of $\Gamma$ loops on $M$ .
$\delta$	Angle of the turbine array with respect to the earth parallels, required to locate each turbine.
$N_R, N_C$	Number of rows and columns of the turbine array.

$\theta$	Angle of the wind velocity vector with respect to the earth parallels.
$w_L$	2D trapezoidal region, symmetric w.r.t. $x$ axis, representing the wake of an $x$ -directed wind, after passing a turbine located at $(0,0)$ .
$w$	trapezoidal 2D region in $R^2$ , representing the wake of a turbine placed at general $(x,y)$ coordinates and facing a general wind direction $\theta$ .
$w_D$	discrete or pixel image of generally positioned wake $w$ .
$\eta$	Wake velocity deficit function $\eta : w_L \rightarrow [0, 1]$ described in the local coordinates of a turbine located at $(0,0)$ with wind pointing in the positive $x$ direction.
$\lambda$	Wake velocity deficit function $\lambda : w \rightarrow [0, 1]$ , for a particular turbine working position and orientation, expressed in the $\Pi$ plane coordinates $(XY)$ .
$\lambda_d$	Digitized version of the function $\lambda$ ( $\lambda_d : w_D \rightarrow \mathbb{N}$ ) with velocity deficit expressed in natural numbers.
$\Lambda$	Superposition of the digitized velocity deficits $\lambda_d(p)$ for all turbine sites $p \in S$ which are contained in the polygonal region $\Gamma$ .

**1. Introduction**

The need for sustainable clean energy sources is a self - evident pre-condition for a minimal societal surviving organization. Wind energy is one of such clean sustainable energy sources. In spite of political oscillations, it is reasonable to expect that wind energy will remain an important participant in the satisfaction of such demands.

The computer simulation of wind energy production is relevant for the technical and economic planning of wind energy facilities. Technical factors for such simulations include but are not limited to terrain, wind, turbine type, energy flow, energy storage, etc., and their interactions.

Investigators' efforts to develop increasingly inclusive models collide with the sheer amounts of data that computational fluid and thermo - dynamics entail. Although from the theoretical point of view many of the aforementioned factors can be considered, that is not the case from the practical point of view.

Examples of the complexities inherent to those factors are: (a) for terrain modeling, the pairing TIN terrain models with wind and wake altitude properties, (b) for turbine types, the coupling of energy extraction and wind behavior in the rotor and wake, (c) for energy flow, the reliability of and the intervals of technically useful wind conditions. (d) for energy storage, the patterns of wind conditions coupled with the capacity of energy storage, transport, consumption, etc. Since an increasingly inter-connected model is impractical, simplifications are conducted.

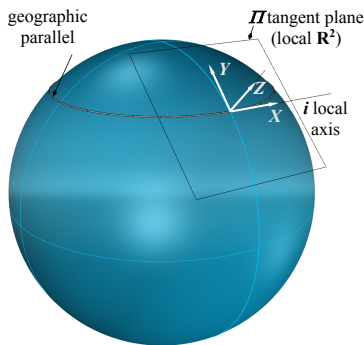


**Figure 1:** Wind Farm location with XY ( $\mathbb{R}^2$ ) Plane Tangent to Earth.

Fig. 1 illustrates that wind farm terrain geographic coordinates usually correspond to the XY plane locally tangent to an ideal earth sphere model. Fig. 3 illustrates the complexity of the interaction among the multiple turbine wakes in a wind farm. The complexity is compounded by the irregular boundaries and exclusion zones of the terrain. The explicit vector (i.e. real-valued) computation of the boolean 2D interactions among the wakes is very expensive, due to the increasing fragmentation as additional turbines are considered. In addition, such a computing effort is not really worthy because the wake model itself is an approximation. This scenario makes pointless the exact polygonal computing. The terrain model upgrade from 2D to 3D would only increase the difficulty and lack of motivation to pursue the vectorial computation.

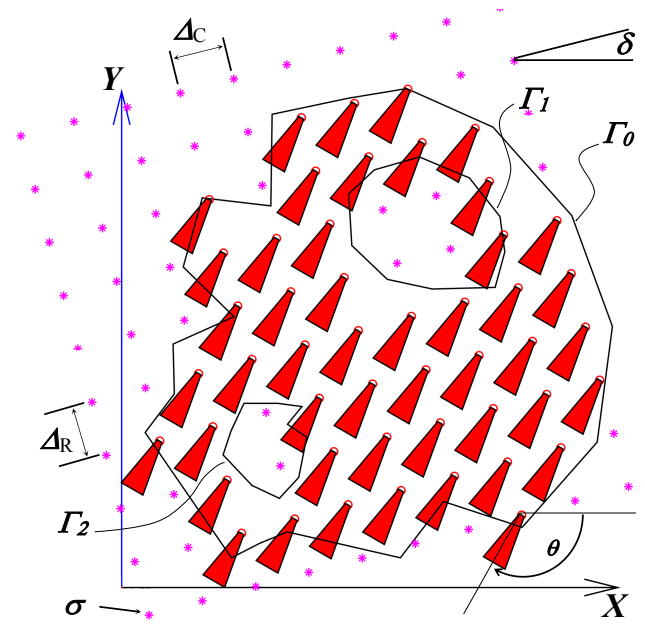


**Figure 2:** Terrain and set of w turbine wakes.  $\sigma$ : turbine array origin,  $\delta$ : orientation of the turbine array,  $\theta$ : wind direction,  $\Delta$ : turbine separation,  $\Gamma$ : terrain boundaries.

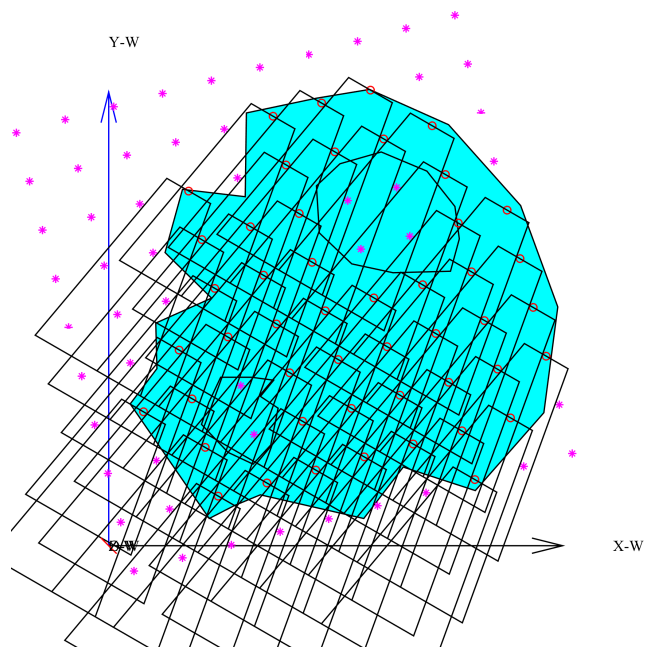


**Figure 3:** Fragmentation of vector (i.e. real - valued) polygon wake model.

In this manuscript, we present a model for optimization of energy production of a wind turbine farm. We fix the turbine used (model and dimensions). Our model is able to accommodate a general polygonal terrain (with convexities and forbidden areas). We use a 3D triangle representation of the terrain, although we do not include 3D calculations in the wind wake. We take into consideration the cross influence of wakes among the wind farm turbines by using a discrete (i.e. pixel or raster) approximation of the correlation among the turbines, as opposed to the explicit calculation of boolean operations among 2D wake profiles (Figs. 3 and 2). We show that the pixel model is simple enough to compute, and flexible enough to simulate the interactions of large numbers of turbines.

## 2. Literature review

This Literature Review seeks to determine whether or not (discrete or analog) graphical models have been used to model the power produced by a wind turbine farm. Analytical models for one turbine wake are already limited by the Fluid Dynamics complexity of the phenomenon. Proportional complexity is present in multi-turbine interaction and turbine - terrain interaction. Turbine farm power modeling has been discussed in the scenario of power maximization and fatigue prevention.

[CLJS13] uses an analytical - heuristic fluid dynamics method for the estimation of turbine wake phenomena, considering different hub heights. This work seeks to maximize power and minimize cost/power by using genetic algorithms. The terrain and initial guess for the array of turbines are rectangular. No attempt is made to take advantage of a graphical approximation.

[MPD94] and [GHA05] use genetic algorithms to minimize the cost per energy unit and to maximize the produced power per surface, respectively, in a rectangular terrain.

[CSHZ13] uses heuristic linear wake model, power law curve, Weibull distribution and profit function in a greedy approach competing against bionic and genetic algorithms to optimize the turbine location problem in a rectangular terrain. The manuscript does not seek a complex wake - wake or wake - terrain model.

[WVYZ10] uses particle swarm optimization (PSO) for micro-siting in wind farms. This work uses turbine separation heuristics. The wake and power model is the usual heuristic one, with no particular contribution, since the emphasis is on the advantage of PSO on classical binary-coded genetic algorithms.

[YZSZ15] discusses a fuzzy genetic as improvement to genetic algorithm. The reference uses terrain iso-height maps, but no emphasis is made on wake interaction with terrain. The model is analytical with heuristics which include but are not limited to terrain roughness. No attempt is made on using discrete graphical modeling.

[GBB\*07] and [WCC\*14] serve as a theoretical basis for the software in [UVG\*15]. This software uses Jensen model [Jen83] and takes into account air density, wind hysteresis, rotor equivalent wind speed, icing conditions, etc. All these references apply fluid dynamics and heuristic formulations for the calculation of the wind farm. In particular, they do not enter into the terrain modeling, and or a discrete graphics approximation of the wake interaction.

[ZSM18] uses a pseudo-random number generation method to optimize the wind farm layout. [WVY\*12] applies Gaussian Particle Swarm Optimization combined with a local search strategy. [MLP08] detects the optimal placement of wind turbines with the help of a Monte Carlo Simulation. In [KS10], a multi-objective evolutionary strategy algorithm is developed to solve the optimization problem. [PMG13] uses two steps for the optimization, starting with a heuristic method to find a convenient starting point and a nonlinear mathematical programming technique to obtain a local optimum. [CSHZ13] takes advantage of a greedy algorithm in order to optimize the wind farm layout. These complex mathematical techniques achieve a result very close to the optimum. But still they are applying the optimization on a regular square area.

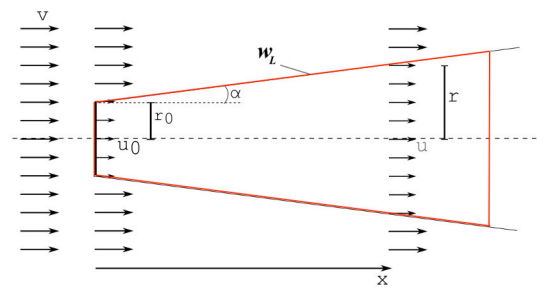


**Figure 4:** Turbine Wake in Local Coordinates ([Jen83]).  $v$ : incoming wind speed (local  $x$  direction).  $u(x,y)$ : internal wake velocity.  $\eta : w_L \rightarrow [0, 1]$ : velocity deficit  $\eta(x,y) = 1 - \frac{u(x,y)}{v}$ .

[CGCP12] discusses flow through a perforated disc as similar to the one through a turbine. It shows that the model gives results similar to direct wind turbine models. The reference mentions but does not discuss multiple turbine wake interactions, nor uses graphical methods to model them.

[FBP\*06] presents an extraordinarily complex analytical fluid dynamics model for the wake, even considering that no terrain is present (off shore scenario). In spite of its complexity, a large number of assumptions are made, since this is an inherently difficult problem. No attempt is made to use graphic discretization to offset such complexities.

[HGH14] simplifies the input factors by only using two fixed wind directions and a non mathematical approach to optimize the wind farm layout. It has the advantage of an irregular grid but the disadvantage of considering a regular area. This reference remarks the need for wake terrain interaction modeling not only to increase power output but to protect turbines from damage. The reference resorts to the 3D-5D heuristic for turbine placement and makes no attempt to use a graphical discrete approximation for calculations.

[NPA15] presents an empirical / analytical fluid dynamics model for turbine wake interactions. the model uses empirical values for wake growth and local turbulence. The reference states future work in modeling a wider range of flow conditions. No attempt is made on using graphical methods for the wake interaction.

[AC17] presents a model optimization of offshore wind farms taking into consideration electrical losses and wake effects. The

wake fluid dynamics model is heuristic - analytical. It uses micro-sitting, in which square array cells are set of containing each turbine, and a fine tuning with discrete subdivisions is conducted. The model pre-determines square cells according to the 3D-5D heuristics (to avoid interaction among neighboring turbines). No attempt is made to take advantage of graphical methods for wake turbine interaction.

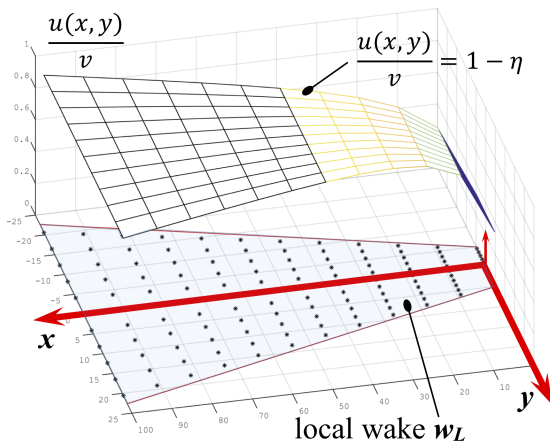


**Figure 5:** Ratio  $\frac{u(x,y)}{v}$ , velocity deficit  $\eta$  and Local Wake. Wind blows in the  $x$  direction.

[BLM14] optimizes (using Monte Carlo methods) the wind farm energy production by locating the turbines. For verification, it conducts wind tunnel experiments. The rectangular site is covered with an array of 100 cells, each optionally containing a turbine. A windward and crosswind distance heuristic is used to define turbine separation. An analytical / heuristic fluid dynamics model is used for power production. No attempt is made to use a discretized graphic representation of the wind wakes or farm.

[GW13]) uses edge detection in images, for synthesizing and compressing polygonal terrain boundaries used in Particle Swarm Optimization of the wind farm layout. The terrain boundary is irregular. The prescribed turbine sites are random too. The wake computation requires the boolean operations among a large number of 2D polygons. Thus, the potential of discrete graphical representation continues to be under - exploited. .

[XYL\*13] presents a Cross Particle Swarm Optimization (CPSO) to optimize the micro-sitting layout for a given wind farm. For the wake modeling, a heuristic minimal distance between 2 turbines is applied. The Z coordinates of terrain are applied in analytic - heuristic wake models. No attempt is made to take advantage of discrete graphical approximations.

## 2.1. Conclusion of literature review

The reviewed literature shows that even with the slightest variation of the modeled phenomena, the models to predict the power output in a wind turbine become extremely complicated. In both extremes, empirical and highly mathematical fluid dynamics methods, the authors use heuristics and thumb rules to make tractable the problem.

Complication mounts with multi - turbine and terrain - turbine interactions, along with transition from 2D to 3D models.

The simplifications generally used for power and wake modeling include: rectangular terrain areas, pre-defined approximate grids (micro- sitting ), turbine separation heuristics (e.g. the 3D-5D thumb rule). We have found very scarce usage of discrete graphical models for wake (and thus power) modeling.

Accordingly, we present in this manuscript the implementation of a pixel - based turbine wake interaction model, in irregular boundary terrains. We show its usefulness for turbine farm power computation, in the context of a wind farm layout optimization.

We apply a fractional factorial Design of Computer Experiments (DOCE) in order to explore conceptual designs of wind farms. The example seeks to find configurations that maximize projected power generation. Yet, it is not our intention to contribute in the specific field of wind farm optimization. Instead we aim to demonstrate that a discrete graphical representation of the turbine wake and wake-terrain interaction has a very important potential for helping an ever more accurate modeling in wind energy production.

## 3. Methodology

This section discusses how the power produced by a wind turbine farm is approximated by discrete models, and as an application, how the power output optimization is thus enabled. The power output for a particular configuration is calculated as follows: (1) The velocity deficit function  $\eta()$  for the turbine type is calculated (Fig. 4) in the local polygonal coordinates of the turbine wake. (2) Each turbine site of the turbine array is tested for inclusion in the farm boundary  $\Gamma$ , thus allowing only turbines inside the terrain (Figs. 2, 7). (3) For each turbine, wake and velocity deficit function are transformed to its actual position in the terrain (Fig. 2) by using 2D transformations (scaling, rotation, translation), (4) The velocity deficits of all turbines are expressed and stored in color discrete levels. (5) The polygonal wakes of the turbines are approximated (Fig. 6) using pixel sets. (6) Each turbine pixel wake is super - imposed onto the overall farm wake pixel array. (7) The full Power of the wind turbine farm is estimated using the pixel-based cross-influenced velocity deficit. (8) The tuning parameters  $\delta$ ,  $\Delta_C$ ,  $\Delta_R$ ,  $N_C$ ,  $N_R$  are modified, if needed, to seek a higher power output. (9) The optimization is stopped when only marginal power improvements are achieved via tuning variable modifications.

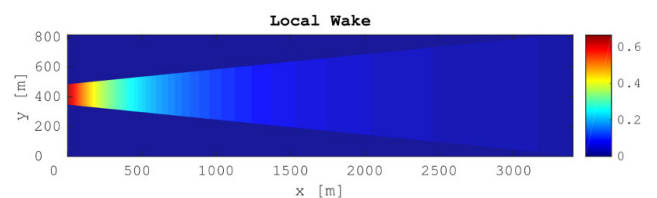


**Figure 6:** Discretized local velocity deficit  $\eta_d$ . V136-3.45MW wind turbine wake. Rotor diameter  $d_{Rotor} = 136$  mt. Entrainment angle  $\alpha = 5.7^\circ$ . Wake length  $L = 25 \cdot d_{Rotor}$ .  $f_x = 1$  mt/pixel).

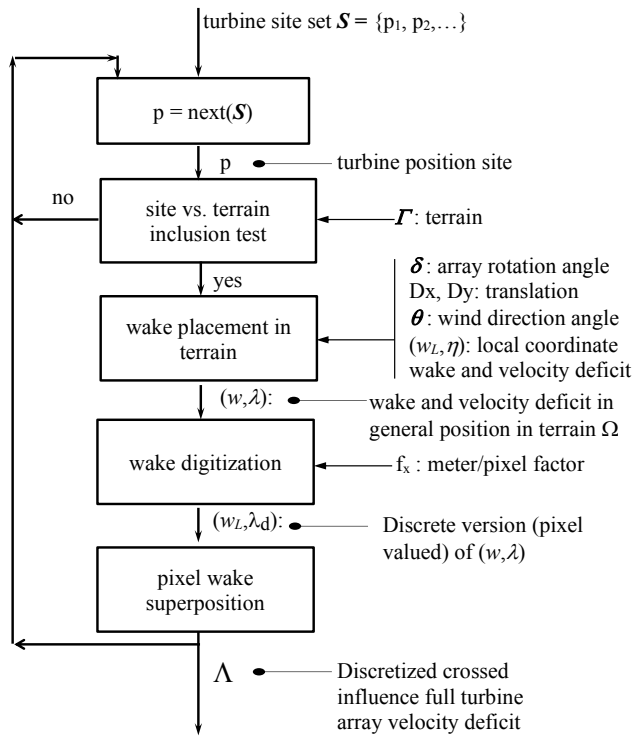


Figure 7: Flow Chart for Pixel Approximation of the Velocity Deficit of the Overall Turbine Farm.

3.1. Variables and assumptions

This section discusses the parameters and variables of the optimization pursued. It also describes the wind turbine specifications. For the purposes of this manuscript, the tuning variables used to maximize the wind turbine farm power output  $P_{farm}$  appear in Table 1.

Variable	Specification
$\delta$ :	Angle of the wind turbine array orientation w.r.t. local parallel.
$\Delta_C$ :	Turbine separation in row direction.
$\Delta_R$ :	Turbine separation in column direction.
$N_C$ :	Number of turbines per column.
$N_R$ :	Number of turbines per row.

Table 1: Tuning Variables of the Turbine grid:  $G = (\delta, \Delta_C, \Delta_R, N_C, N_R)$ .

Computer simulation (fixed) parameters and characteristics of the wind turbine appear in tables 2 and 3, respectively.

3.2. Wake Transformation.

The 2D geometric transformations discussed in this project are used to: (1) rotate and translate the basic local wake function

Parameter	Specification
$\Omega$	Polygonal 3D Terrain, with holes and concavities.
$\vec{v}$	Wind vector with speed $v =  \vec{v} $ . $\vec{v} = [v_x, v_y, 0]$ and $\theta = \angle(\vec{v}, \hat{i})$ . In this investigation, it is considered that the terrain $\Omega$ is small enough to be exposed to a uniform wind condition.
$N_{max}$	Maximum number of available wind turbines.
$\sigma$	Origin of the turbine array inside the terrain $M$ ( $\sigma \in \mathbb{R}^2$ ).

Table 2: Power Optimization (fixed) Parameters.

Characteristic	Meaning	Value
Turbine Type	Wind	Vestas V136-3.45MW
$r_0$ :	Rotor radius	68 m
$P_{rated}$ :	Rated power production	3.45 MW
$v_{cut,in}$ :	Cut in wind speed	3 m/s
$v_{cut,out}$ :	Cut out wind speed	22.5 m/s

Table 3: Wind Turbine Specification.

$\eta: \mathbb{R}^2 \rightarrow [0, 1]$  to place  $\eta()$  in the particular position and orientation of that wind turbine inside the polygonal region  $\Gamma$ , resulting in the positioned red wakes (Fig.2) supporting the deficit  $\lambda()$  functions. (2) scale and truncate the real - valued red wake supports for  $\lambda()$  functions into a pixel discretization of Fig.2.

Notice that the real - valued deficits  $\lambda()$  are also converted to a subset of  $\mathbb{N}$ , which in this manuscript is a color map. The resulting functions  $\lambda_d$  have both discrete trapezoid-like support and also discrete value  $\lambda_d(k)$  for pixel  $k$ . The sequence of 2D geometric transformations (in homogeneous form) used here:

1. To orient the wake with the wind direction  $\theta$ :

$$T_1 = \begin{bmatrix} \cos(\theta) & -\sin(\theta) & 0 \\ \sin(\theta) & \cos(\theta) & 0 \\ 0 & 0 & 1 \end{bmatrix} \quad (1)$$

2. To locate the  $(l, m)$  turbine in the array, with parameters  $(\delta, \Delta_C, \Delta_R, \sigma)$ :

$$T_2 = \begin{bmatrix} 1 & 0 & \sigma_x \\ 0 & 1 & \sigma_y \\ 0 & 0 & 1 \end{bmatrix} \cdot \begin{bmatrix} C(\delta) & -S(\delta) & 0 \\ S(\delta) & C(\delta) & 0 \\ 0 & 0 & 1 \end{bmatrix} \cdot \begin{bmatrix} 1 & 0 & (l-1) \cdot \Delta_C \\ 0 & 1 & (m-1) \cdot \Delta_R \\ 0 & 0 & 1 \end{bmatrix} \quad (2)$$

3. To map real - value coordinates of Fig. 2 to pixel values.

$$T_3 = \begin{bmatrix} (1/f_x) & 0 & 0 \\ 0 & (1/f_x) & 0 \\ 0 & 0 & 1 \end{bmatrix} \quad (3)$$

4. To produce the discretization of the real - valued wake map by

using a truncated transformation sequence  $T = [(T_3 \cdot T_2 \cdot T_1)]$ , with  $\lceil \cdot \rceil$  being the **round** operator.

Notice that the turbine array orientation  $\delta$  influences the spot in which a turbine is located while the  $\theta$  angle influences its orientation.

### 3.3. Wake model.

This manuscript applies the 2-dimensional N.O. Jensen model [Jen83] for the velocity deficit, with the following assumptions: (1) No thrust forces are considered in the wind momentum balance. (2) The wake is represented by a 2D trapezoid polygonal region. (3) The velocity deficit function inside the wake depends on the distance  $x$  to the rotor plane as per Eq. 5 and Fig. 4. The gaussian wind velocity distribution vertical to the wind direction in  $y$  direction is transformed into a "top-hat" distribution. This deletes the influence of  $y$  on the wind velocity inside of a wake.

$$\eta(x,y) = 1 - \frac{u(x,y)}{v} \tag{4}$$

$$\eta(x,y) = \left\{ 1 - \frac{2}{3} \cdot \left( \frac{r_0}{r_0 + \alpha \cdot x} \right)^2 \right\} \tag{5}$$

with  $\alpha$  as entrainment factor of the wake,  $v$  as incoming wind speed and  $r_0$  as rotor radius. The used model prescribes that  $\eta()$  is independent of  $y$ . The wake effect extends a distance of  $L$  (in the local  $x$  direction). Thus, the maximal wake width, at  $x = L$ , is  $W = 2 \cdot L \cdot \tan(\alpha) + d_{Rotor}$ .

For the turbine in site  $j$ , The velocity deficit resulting from being affected by the wakes of the other turbines is:

$$\Lambda(j) = \sqrt{\sum_{i \in W(j)} \lambda_i^2} \tag{6}$$

with  $W(j)$  being the set of turbines affecting the wind velocity at position  $j$  ([KS10]).

### 3.4. Turbine Power Output

Fig. 6 shows a pixel approximation of the lost of kinetic energy in the wind, within the turbine wake (Jensen model [Jen83], Fig. 4). The turbine is located in the (0,400) coordinate of Fig. 6, and the wind flows in the positive  $x$  direction. The wake neighborhood near (0,400) shows a high value (red) of the drop -or deficit- in wind kinetic velocity. At  $x = 0$ , the wind has just transferred much of its kinetic energy to the turbine. As the wind moves increasing its  $x$  coordinate, its velocity recovers, eventually equaling the free wind velocity (blue).

The power output for the wind farm is computed using the pixel superposition of the velocity deficit wakes  $\Lambda_i$ , for each turbine  $i$  present in the domain  $(M, \Gamma)$ , as follows:

1. Compute turbine  $i$  pixel - based velocity deficit  $\eta$  in the turbine local coordinates, producing the discrete approximation of Fig. 6. Notice that turbine  $i$ , and their model, may be different from the other ones. This fact also opens the opportunity to consider turbine and terrain altitude in the following investigations.

2. By using the geometric transformations in section 3.2, transform the pixel approximation of (1) to be located in the locii actually contained in the terrain  $(M, \Gamma)$ , and oriented with the wind. The pixel wake is correctly located in the terrain scenario, but alone.
3. Super-impose the velocity deficits of the whole turbine set (Eq. 6), to obtain the full cross-influence pixel array in Fig. 9(a).
4. By using the super-imposed discrete velocity deficit map of Fig. 9(a), compute the velocity in front of turbine  $i$ . For turbine  $i$ , it means to average  $\Lambda(k)$  over the pixels  $k$  immediately in front (with respect to the wind direction) of turbine  $i$ :

$$\eta_i = \text{avg}_k(\Lambda_k) \tag{7}$$

5. Compute the wind velocity immediately in front of turbine  $i$ :

$$u_i = v(1 - \eta_i) \tag{8}$$

6. Compute the power output  $P_i = P(u_i)$  for turbine  $i$  from Fig. 8.

Eq. 9 accumulates the contributions of all turbines present in the wind turbine farm  $(M, \Gamma)$ .

$$P = \sum_i P_i \tag{9}$$

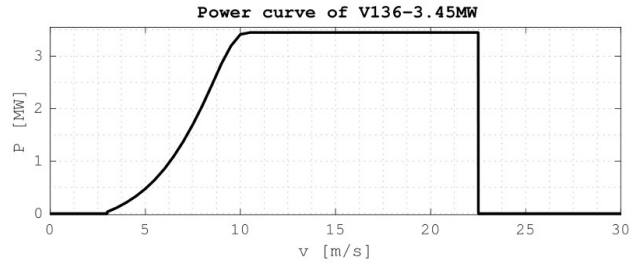


Figure 8: Power curve of the Vestas V136-3.45MW wind turbine.

### 3.5. Optimization Methodology

To explore different conceptual design scenarios, a  $2^{5-3}$  DOCE with an external array of  $2^2$  with a center point ( $2^2 + 1$ ) was conducted. Its goal is to gauge the influence on the wind turbine farm power output ( $P_{farm}$ ) of the variables: (a) the angle  $\delta$  of the wind turbine array orientation with respect to the parallels, (b) turbine separation in the row and column directions ( $\Delta_c$  and  $\Delta_g$ , respectively), and (c) the number of turbines per column and per row ( $N_C$  and  $N_R$ , respectively). Notice that wind velocity vector direction ( $\theta$ ) and magnitude ( $\|v\|$ ) are variables from the environment that cannot be controlled. For this reason, they are considered to be parameters. We use Daniel Plots to identify the most significant process variables, with a single replicate per treatment while using the external  $2^2 + 1$  DOCE to yield 5 responses/treatment for power  $P_{farm}$  at each one of the conditions for the wind velocity vector.

4. Results

4.1. Pixel approximation of power computation

Fig. 2 displays the vectorized (i.e. real-valued) computation to identify and locate the turbines within the polygonal terrain  $\Gamma$ . The wakes are in this figure displayed as red filled trapezoids, oriented according to the wind velocity. This computation yields the  $\lambda$  (Fig. 7) velocity deficits properly located in the terrain.

Fig. 9(a) presents the result of super-imposed wake velocity deficits, expressed in discrete manner. This discretization involves both (a) pixelation of the wakes over the domain and (b) representation of the velocity deficit using integer numbers (in this case, colors). This figure includes only turbines which fall inside the domain  $\Gamma$ .

Fig. 9 shows the texture map of the overall velocity deficits in pixel format, over the 3D terrain  $M$ . The projection also includes the boundary  $\Gamma$ .

4.2. Conceptual Geometric Design of a Wind Turbine Farm

This section shows the application of the discretized cross - correlated image of the velocity deficits of the turbine farm, in the optimization of the power output  $P$  of the wind turbine farm. Two strategies are conducted: (a) Fractional Factorial Design and (b) Gradient.

4.2.1. Fractional factorial design of experiments

This optimization problem is stated as follows:

- Optimize:** the power  $P$  of the wind turbine farm.
- Tuning Variables:**  $\delta, \Delta_C, \Delta_R, N_C, N_R$ .
- Constant Parameters:**  $\Omega, M, \Gamma, \vec{v}, \theta, N_{max}, \sigma$ , Turbine type.

4.2.2. Conceptual Design of Wind Turbine Farms

The pixel approximation of power computation algorithm is applied to several conceptual design scenarios constructed using a fractional factorial DOCE as shown in Table 4.

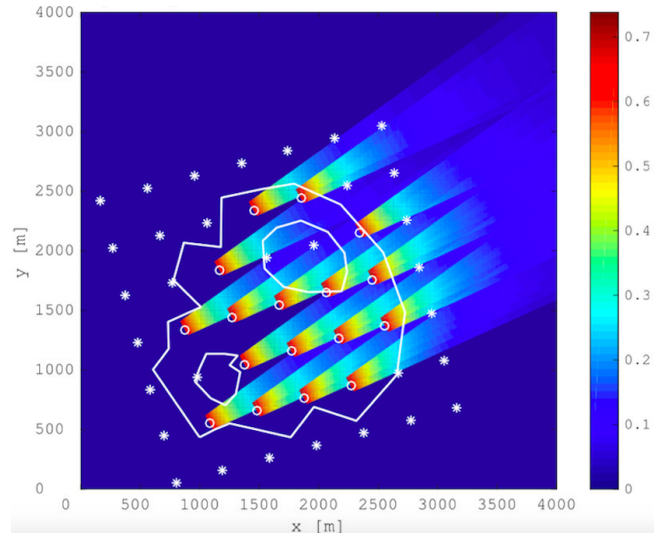
4.2.3. Gradient - based Optimization

This optimization problem is stated as follows:

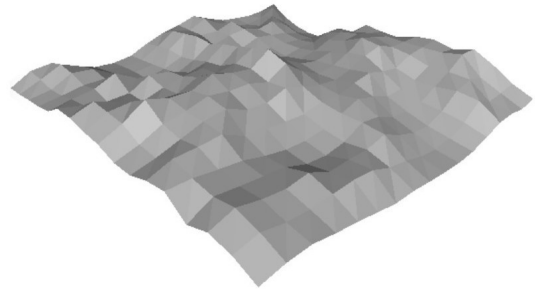
- Optimize:** the power  $P$  of the wind turbine farm.
- Tuning Variables:**  $\delta, \Delta_C = \Delta_R \in [2 \cdot d_{Rotor}, 10 \cdot d_{Rotor}]$
- Constant Parameters:**  $\Omega, M, \Gamma, \vec{v}, \theta, N_{max}, N_C, N_R, \sigma$ , Turbine type.

5. Conclusion and future work

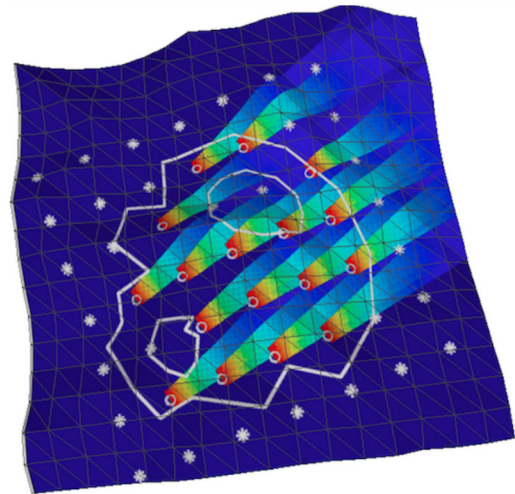
This manuscript presents the implementation of a discrete - value methodology for calculation of the cross - correlated velocity deficits of a wind turbine farm. The discrete value approximation of the velocity deficit spatial distribution on the terrain  $\Omega$  is applied on both the terrain and on the values of the velocity deficits. This methodology allows a significant simplification of the computing, since eliminates the staggering polygon fragmentation that occurs



(a) 2D image of pixel - based wake map with full wind farm interaction and terrain boundary restriction.  $\theta = 30^\circ, \delta = 15^\circ, \Delta_R = \Delta_C = 3 \cdot d_{Rotor}$ .



(b) 3D Terrain  $M$  in Triangle Mesh Format (in this case, a TIN data set).



(c) Texture map of the 2D overall velocity deficit of Fig. 9(a) onto the terrain triangular mesh of Fig. 9(b).

**Figure 9:** 2D Overall Velocity Deficit of Wind Farm and its Map (projection) onto the 3D Terrain.

					$\delta^\circ$	-1 (0)	-1 (0)	1 (90)	1 (90)	0 (45)
					$v0$ (m/s)	-1 (4)	1 (20)	-1 (4)	1 (20)	0 (12)
TREAT - MENT	$\Delta_C$ (m)	$\Delta_R$ (m)	$\theta^\circ$	$N_R$	$N_C$					
1	-1 (250)	-1 (250)	-1 (0)	1 (7)	-1 (1)	1,48	169,04	1,48	169,04	85,89
2	1 (1250)	-1 (250)	-1 (0)	-1 (1)	-1 (1)	0,21	3,45	0,21	3,45	3,41
3	-1 (250)	1 (1250)	-1 (0)	-1 (1)	1 (7)	0,21	24,15	1,48	24,15	23,90
4	1 (1250)	1 (1250)	-1 (0)	1 (7)	1 (7)	1,48	24,15	1,07	24,15	23,90
5	-1 (250)	-1 (250)	1 (90)	1 (7)	-1 (1)	0,21	24,15	1,48	24,15	23,90
6	1 (1250)	-1 (250)	1 (90)	-1 (1)	-1 (1)	1,48	24,15	1,07	24,15	23,90
7	-1 (250)	1 (1250)	1 (90)	-1 (1)	1 (7)	0,21	3,45	0,21	3,45	3,41
8	1 (1250)	1 (1250)	1 (90)	1 (7)	1 (7)	7,48	169,05	7,48	169,05	158,97

Table 4: Results of Conceptual Design Scenarios.

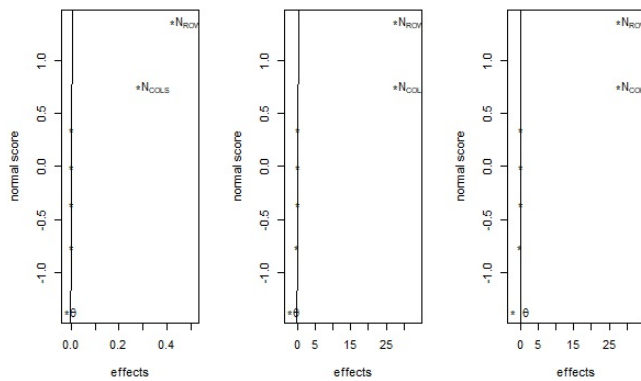


Figure 10: Daniel Plot for screening of dominant variables ([Dan59]) showing as dominant:  $N_R$ ,  $N_C$ ,  $\theta$ .

Characteristic	Observation
$\delta$	interval $[0^\circ, 90^\circ]$ , step $2^\circ$
$\Delta_C = \Delta_R$	interval $[2 \cdot d_{Rotor}, 10 \cdot d_{Rotor}]$
$N_C$	3 turbines
$N_R$	4 turbines
$v$	10 m/s
Size of Terrain $M$	$3500 \times 3500$ m
$\delta$ start	$22^\circ$
$\Delta_R$ start	$7 \cdot d_{Rotor}$

Table 5: Parameter Values for Optimization of Turbine Farm Power Using Gradient.

when real - valued polygonal representations of the wakes are used. The velocity deficits are mapped to colors, and therefore, the wake superpositions are computed as operations on images. Although the image operations represent a significant opportunity for application of graphics hardware, the main advantage of the discretization approach is to allow far greater complexity in the modeling of the terrain that hosts the turbine farm. This article demonstrates that polygonal terrains with holes or excluded regions are completely feasible. In addition, the terrain itself may be represented in 3D

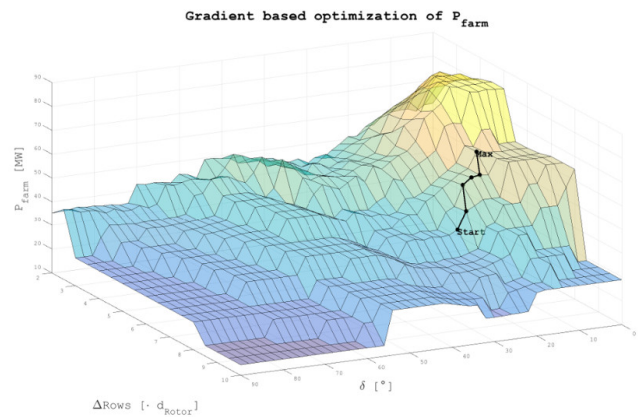


Figure 11: Gradient Maximization Path for  $P = P(\delta, \Delta_R)$  as per Table 5. Local maximum found at  $(\delta, \Delta_R) = (12^\circ, 6 \cdot d_{Rotor})$ .

(e.g. TIN format of Geographic Information Systems). All these features would be absolutely out of question if real - valued polygonal representations for turbine wakes are used.

Significant opportunities are opened by using discrete wakes and velocity deficits. For example, wake models may be considered which include altitude interaction turbine/terrain, mixed turbine types are possible, use of parallel Graphic Processing Units (GPU) are able to accelerate the computations. Other graphic methods (e.g. 2D ray tracing or plane sweeping) can be explored, since they have significant improvements in the speed and accuracy aspects. Additional types of turbine farm power optimizations would be possible (e.g. with random turbine locations).

References

[AC17] AMARAL L., CASTRO R.: Offshore wind farm layout optimization regarding wake effects and electrical losses. *Engineering Applications of Artificial Intelligence* 60 (2017), 26 – 34. doi:https://doi.org/10.1016/j.engappai.2017.01.010.  
 [BLM14] BRUSCA S., LANZAFAME R., MESSINA M.: Wind turbine placement optimization by means of the monte carlo simulation method.



- Modelling and Simulation in Engineering 2014* (2014), 8. Article ID 760934. doi:<http://dx.doi.org/10.1155/2014/760934>.
- [CGCP12] CRASTO G., GRAVDAHL A., CASTELLANI F., PICCIONI E.: Wake modeling with the actuator disc concept. *Energy Procedia 24* (2012), 385 – 392. Selected papers from Deep Sea Offshore Wind RD Conference, Trondheim, Norway, 19-20 January 2012. doi:<https://doi.org/10.1016/j.egypro.2012.06.122>.
- [CLJS13] CHEN Y., LI H., JIN K., SONG Q.: Wind farm layout optimization using genetic algorithm with different hub height wind turbines. *Energy Conversion and Management 70* (2013), 56 – 65. doi:<https://doi.org/10.1016/j.enconman.2013.02.007>.
- [CSHZ13] CHEN K., SONG M., HE Z., ZHANG X.: Wind turbine positioning optimization of wind farm using greedy algorithm. *Journal of Renewable and Sustainable Energy 5*, 2 (2013), 023128.
- [Dan59] DANIEL C.: Use of half-normal plots in interpreting factorial two-level experiments. *Technometrics 1*, 4 (1959), 311–341.
- [FBP\*06] FRANDSEN S., BARTHELMIE R., PRYOR S., RATHMANN O., LARSEN S., HOEJSTRUP J., THOEGERSEN M.: Analytical modelling of wind speed deficit in large offshore wind farms. *Wind energy 9*, 1-2 (2006), 39–53. "doi: 10.1002/we.189".
- [GBB\*07] GRYNING S., BATCHVAROVA E., BRUEMMER B., JOERGENSEN H., LARSEN S.: On the extension of the wind profile over homogeneous terrain beyond the surface boundary layer. *Boundary-Layer Meteorology 124*, 2 (2007), 124: 251. doi:<https://doi.org/10.1007/s10546-007-9166-9>.
- [GHA05] GRADY S., HUSSAINI M., ABDULLAH M.: Placement of wind turbines using genetic algorithms. *Renewable energy 30*, 2 (2005), 259–270.
- [GW13] GU H., WANG J.: Irregular-shape wind farm micro-siting optimization. *Energy 57* (2013), 535–544.
- [HGH14] HUA Z., GU Y., HOU C.: Wind farm micro-siting optimization and benefits analysis. *Advanced Materials Research 1055* (2014), 389–393.
- [Jen83] JENSEN N.: *A note on wind generator interaction*. Technical University of Denmark, Riso National Laboratory, 1983. M-2411.
- [KS10] KUSIAK A., SONG Z.: Design of wind farm layout for maximum wind energy capture. *Renewable energy 35*, 3 (2010), 685–694.
- [MLP08] MARMIDIS G., LAZAROU S., PYRGIOTI E.: Optimal placement of wind turbines in a wind park using monte carlo simulation. *Renewable energy 33*, 7 (2008), 1455–1460.
- [MPD94] MOSETTI G., POLONI C., DIVIACCO B.: Optimization of wind turbine positioning in large windfarms by means of a genetic algorithm. *Journal of Wind Engineering and Industrial Aerodynamics 51*, 1 (1994), 105–116.
- [NPA15] NIAYIFAR A., PORTE-AGEL F.: A new analytical model for wind farm power prediction. *Journal of Physics: Conference Series 625*, 1 (2015), 012039. URL: <http://stacks.iop.org/1742-6596/625/i=1/a=012039>.
- [PMG13] PÉREZ B., MÍNGUEZ R., GUANCHE R.: Offshore wind farm layout optimization using mathematical programming techniques. *Renewable Energy 53* (2013), 389–399.
- [UVG\*15] UNDHEIM O., VINDTEKNIKK K., GROENSLETH M., BERGE E., IVERSEN E., ROGNLIEN L.: Wind farm simulator; time-dependent wind energy calculations. In *EERA DeepWind 2015* (2015).
- [WCC\*14] WAGNER R., CAÑASADILLAS B., CLIFTON A., FEENEY S., NYGAARD N., POODT M., MARTIN C. S., TÁIJXEN E., WAGENAAR J. W.: Rotor equivalent wind speed for power curve measurement – comparative exercise for ica wind annex 32. *Journal of Physics: Conference Series 524*, 1 (2014), 012108. URL: <http://stacks.iop.org/1742-6596/524/i=1/a=012108>.
- [WWY\*12] WAN C., WANG J., YANG G., GU H., ZHANG X.: Wind farm micro-siting by gaussian particle swarm optimization with local search strategy. *Renewable Energy 48* (2012), 276–286.
- [WWYZ10] WAN C., WANG J., YANG G., ZHANG X.: Optimal micro-siting of wind farms by particle swarm optimization. In *Advances in Swarm Intelligence. ICSI 2010. Lecture Notes in Computer Science*, Tan Y., Shi Y., Tan K., (Eds.), vol. 6145. Springer, Berlin, Heidelberg, 2010, pp. 198–205. doi:[https://doi.org/10.1007/978-3-642-13495-1\\_25](https://doi.org/10.1007/978-3-642-13495-1_25).
- [XYL\*13] XU C., YANG J., LI C., SHEN W. Z., ZHENG Y., LIU D.: A research on wind farm micro-siting optimization in complex terrain. In *Proceedings of the 2013 International Conference on aerodynamics of Offshore Wind Energy Systems and wakes ICOWES2013* (2013), pp. 669–679.
- [YZSZ15] YANG J., ZHANG R., SUN Q., ZHANG H.: Optimal wind turbines micro-siting in onshore wind farms using fuzzy genetic algorithm. *Mathematical Problems in Engineering 2015* (2015), 9. Article ID 324203. doi: "<http://dx.doi.org/10.1155/2015/324203>".
- [ZSM18] ZERGANÉ S., SMAILI A., MASSON C.: Optimization of wind turbine placement in a wind farm using a new pseudo-random number generation method. *Renewable Energy 125* (2018), 166–171.